Journal of Materials Chemistry A

ROYAL SOCIETY OF CHEMISTRY

PAPER

View Article Online
View Journal | View Issue

Check for updates

Cite this: J. Mater. Chem. A, 2024, 12, 7279

Nanoscale stirring at the liquid–liquid interface: the interfacial nano-vortexer actively converges immiscible biphasic reactants for enhanced phase-transfer catalysis†

Zhi Zhong Ang,[a] Veronica Pereira,[a] Siew Kheng Boong,[a] Haitao Li[b] and Hiang Kwee Lee *[acd]

Liquid–liquid biphasic reactions hold great promise for green molecular synthesis by leveraging mild chemicals and reaction conditions that are otherwise challenging in traditional single-phase chemistry. However, current interfacial reaction designs suffer from limited practicality due to the unsustainable use of high catalyst/reactant loadings and halogenated solvents to promote chemical reactions. Herein, we achieve efficient interfacial phase-transfer catalysis using green organic solvent by strategically positioning magnetically active nano-vortexers at the liquid–liquid boundary to effectively manipulate biphasic chemical species at the point-of-reaction. Using the interfacial nitration of phenol as a model reaction, the dynamic spinning of these interfacial nano-vortexers attains an optimal nitrophenol yield of ~90% in just 2 hours. This superior performance represents up to a 200-fold enhancement in phase-transfer catalysis compared to control experiments involving a non-dynamic liquid–liquid interface or traditional homogenization methods. Comprehensive investigations underscore the importance of our design to actively converge and enrich reaction/catalyst species directly at the liquid–liquid interface, thus kinetically boosting phase-transfer catalysis even with the use of dilute concentrations of catalysts and/or chemical reagents. Our unique mass manipulation approach offers valuable insight into achieving efficient interfacial reaction/catalysis to create enormous opportunities in realizing greener chemistries for diverse chemical, environmental, and energy applications.

Received 19th October 2023
Accepted 7th February 2024

DOI: 10.1039/d3ta06360g

rsc.li/materials-a

1. Introduction

Liquid–liquid reaction utilizes the interfacial boundary formed between two immiscible solvents to efficiently bring together reactants with large polarity disparities for molecular transformation.[1–5] This emerging approach notably offers distinct advantages that are challenging to achieve in traditional single-phase chemistry, such as enabling unique reaction pathways with improved efficiency/selectivity[6,7] and the use of greener chemicals/conditions[8–10] for molecular synthesis. Moreover, the interfacial reaction design could also allow parallel separation of reactant and product species into different liquid phases to minimize the need for post-reaction purification.[11,12] This ensemble of benefits is crucial for a broad range of pharmaceuticals, chemicals, and materials applications.[13–15] There are two general approaches to enhance interfacial reactions which mainly focus on facilitating the transportation of reaction species to the thin liquid–liquid interface where the reaction occurs. The first method involves the use of high reactant concentrations to establish a steep concentration gradient for accelerating molecule transfer to the interfacial boundary during chemical reactions.[16,17] Another method utilizes a larger volume of one solvent phase and subsequent mechanical agitation to create emulsions that enhance interfacial contact between the immiscible solvents.[18,19] However, the use of high reactant concentrations and excessive solvents is environmentally unsustainable and uneconomical, and poses severe safety hazards.

Phase-transfer catalysis offers a promising solution to overcome these limitations by chemically binding reactant species in one liquid phase and effectively delivering them into the other liquid phase to kinetically boost the biphasic reaction.[20–22]

[a]Division of Chemistry and Biological Chemistry, School of Chemistry, Chemical Engineering and Biotechnology, Nanyang Technological University, 21 Nanyang Link, Singapore 637371, Singapore. E-mail: hiangkwee@ntu.edu.sg
[b]School of Chemistry and Chemical Engineering, Yangzhou University, Yangzhou, 25002 P. R. China
[c]Institute of Materials Research and Engineering, The Agency for Science, Technology and Research (A*STAR), 2 Fusionopolis Way, #08-03, Innovis, Singapore 138634, Singapore
[d]Centre for Hydrogen Innovations, National University of Singapore, E8, 1 Engineering Drive 3, Singapore 117580, Singapore

† Electronic supplementary information (ESI) available. See DOI: https://doi.org/10.1039/d3ta06360g

Quaternary ammonium salts are commonly chosen as phase-transfer catalysts (PTCs) because of their solubility in both organic and aqueous solutions to facilitate reactant transfer between the immiscible liquid phases.[23–25] Moreover, these systems often employ halogenated organic solvents owing to their higher affinity towards organic catalysts and reactants for enhanced catalysis.[26,27] For instance, the application of PTCs has allowed the mild nitration of phenols using dilute HNO_3 acid instead of strong nitrating agents (*e.g.* mixed acids, concentrated HNO_3) in traditional chemistry.[28,29] Anionic exchange between ammonium salt-based PTCs and HNO_3 facilitates the transfer of nitrate ions (NO_3^-) from the aqueous phase into the organic phase, where the nitration reaction occurs. However, the use of halogenated solvents raises significant environmental/health concerns and requires extensive treatment during disposal.[30,31] Although efforts are made to explore greener organic solvents (*e.g.* ethyl acetate), this approach is impeded by the leaching of PTCs and/or reactants into the aqueous phase which is further exacerbated by mechanical homogenization. The accumulation of vital chemical species in the aqueous non-reaction phase consequently deactivates the biphasic reaction and necessitates high catalyst/reactant loadings to promote the catalysis. These limitations have a severe impact on catalytic efficiency and pose formidable challenges to the practical application of phase-transfer catalysis in chemical processes.

Herein, we achieve efficient phase-transfer catalysis by designing a magnetic-responsive nano-vortexer and strategically incorporating it at the liquid–liquid interface to effectively manipulate chemical species within the immiscible solvents, even with the use of green organic solvents. Our strategy exploits the spinning motion of the interfacial nano-vortexer under a rotating magnetic field to create unique vortex-like hydrodynamic flows that extend into both the aqueous and organic phases. This phenomenon will actively converge biphasic reactants and PTCs towards the nano-vortexer, thereby concentrating chemical species at the liquid–liquid interface to kinetically boost the biphasic reaction. Additionally, we introduce a twin stirring approach that combines nanoscale interfacial stirring through our nano-vortexer with macroscopic stirring using a commercial stirbar. This combination leverages the latter to swiftly deliver chemical species from the bulk solution to the vicinity of the interfacial region for enhanced catalysis. Notably, our unique material approach differs from traditional chemical methods that typically rely on high reactant/PTC concentrations, modification of PTC chemical structures, and/or use of halogenated solvents.

As a proof-of-concept demonstration, we employ the interfacial nano-vortexer to drive the interfacial nitration of phenol due to the importance of nitrophenols as chemical precursors in the fine chemical and agrochemical industries.[32,33] Specifically, we utilize ethyl acetate as the green organic solvent for this model phase-transfer catalytic reaction. The dynamic spinning of our unique design enables efficient interfacial nitration, achieving an optimal nitrophenol yield of ~90% in 2 hours and providing a >200-fold enhancement compared to control experiments involving a non-dynamic liquid–liquid interface. Moreover, this approach surpasses conventional interfacial methods that require a longer reaction duration (~4 h) and employ environmentally harmful halogenated organic solvents. Comprehensive investigations highlight that the interfacial nano-vortexer and twin spinning approach realize efficient biphasic reactions by enabling efficient control over molecule transportation at both the nano- and macroscopic-scales, even when utilizing dilute reactants or PTC concentrations. Our work offers valuable insights into the effective manipulation and enrichment of vital chemical species directly at the point-of-reaction crucial for enhancing interfacial reactions. These findings will contribute to the advancement of environmentally benign and sustainable practices in chemical manufacturing and environmental remediation (*e.g.*, oil pollution).

2. Results and discussion

Our interfacial nano-vortexer plays a vital role in biphasic reactions by dynamically converging immiscible reactants onto a liquid–liquid interface to facilitate efficient molecule interactions and chemical reactions (Fig. 1A). We employ Fe_3O_4@SiO_2 nanochains as the interfacial nano-vortexer due to their strong magnetic properties and chemical robustness. To synthesize Fe_3O_4@SiO_2 nanochains, magnetically active Fe_3O_4 nanoparticles (diameter, 160 ± 34 nm; Fig. S1†) are first pre-aligned into chain-like structures using permanent magnets. These assembled particles are then *in situ* coated with a thin SiO_2 shell (thickness, ~56 nm, Fig. 1B and S2†) through a modified Stöber reaction to preserve the structural integrity of nanochains, even after removing the permanent magnets.[34,35] We further functionalize the SiO_2 shell surface *via* the chemical grafting of (*N*,*N*-dimethylaminopropyl)trimethoxysilane (DMAPTS) onto the SiO_2 shell (Fig. S3†). Attenuated total reflectance infrared (ATR-IR) spectroscopy characterization affirms the successful modification of the surface chemistry of Fe_3O_4@SiO_2 nanochains through the emergence of new stretching bands belonging to DMAPTS (Fig. S4A†).[36,37] Together with their nanoscale size, the surface functionalization of the Fe_3O_4@SiO_2 nanochains is crucial to facilitate their uniform assembly at the interface between the immiscible aqueous and organic phases (*e.g.* ethyl acetate, Fig. 1C and S5†). This is likely due to DMAPTS containing a tertiary amine moiety which enables its interactions with both aqueous and organic phases, thereby allowing the nano-vortexers to disperse evenly across the immiscible liquid–liquid interface. The self-assembly process is driven by the minimization of interfacial free energy through the formation of the liquid–solid–liquid interface.

The ability of the Fe_3O_4@SiO_2 nanochains to spin under a magnetic stimulus is crucial for driving hydrodynamic flows to accelerate molecule transfer from both the organic and aqueous phases towards the liquid–liquid interface. Thus, we investigate the spinning dynamics of Fe_3O_4@SiO_2 nanochains in water and organic liquid (*e.g.* decane) under an applied rotating magnetic field using an optical microscope equipped with a high-speed camera. When subjected to an applied rotating field at 700 rpm, the Fe_3O_4@SiO_2 nanochains exhibit

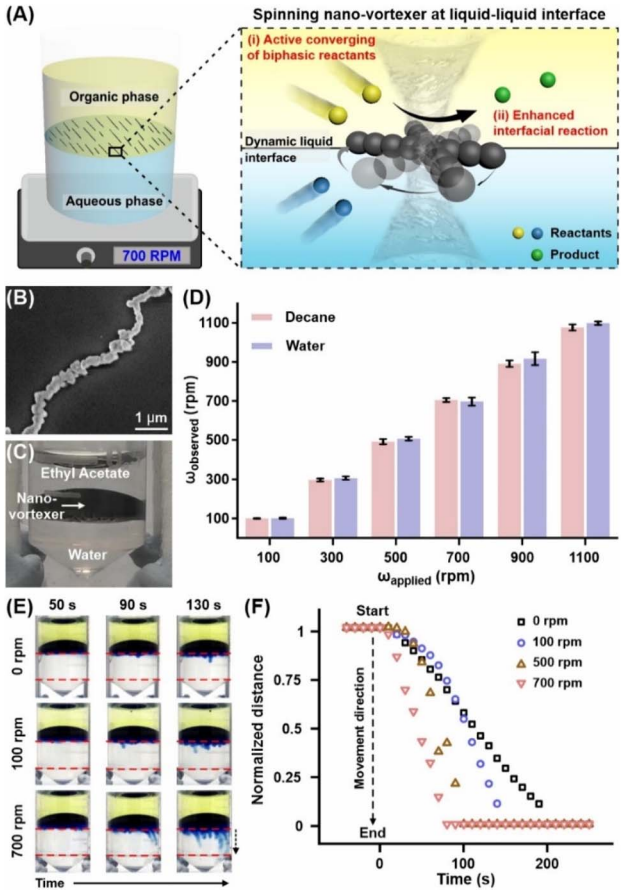

Fig. 1 (A) Scheme depicting the use of an interfacial nano-vortexer at the liquid–liquid interface to boost phase-transfer catalysis. (B) SEM image of the Fe_3O_4@SiO_2 nanochain. (C) Image showing the assembly of Fe_3O_4@SiO_2 nanochains at the water–ethyl acetate interface. (D) Spin rates of the Fe_3O_4@SiO_2 nanochains in decane or water when subjected to an applied magnetic field rotating between 100 and 1100 rpm. (E) Optical snapshots depicting the movement of the dye tracer from the liquid–liquid interface into the underlying aqueous phase when the interfacial nano-vortexer remains stationary or spins at 100 rpm and 700 rpm. (F) Quantitative tracking of the dye tracer as observed in (E).

a distinct spinning motion along their vertical axis and complete a full revolution in ~85 ms (Fig. S6†). This observation highlights the synchronous spinning of Fe_3O_4@SiO_2 nanochains with the applied magnetic field to achieve an effective rate of ~700 rpm. Moreover, the spin rate of nanochains in both decane and water can be easily programmed between 100 rpm and 1100 rpm by modulating the applied rotating magnetic field (Fig. 1D). The nanochain assembly and its spinning motion also remain stable over an extended duration of up to 2 hours (Fig. S7†). These characteristics are key to enabling the effective utilization of Fe_3O_4@SiO_2 nanochains as interfacial nano-vortexers in biphasic reactions.

Having demonstrated the effective spinning of the Fe_3O_4@SiO_2 nanochains, we examine their potential application as interfacial nano-vortexers at the boundary between organic and aqueous liquids. To investigate the effect of interfacial rotation on hydrodynamic flow in bulk solutions, we employ an indirect colorimetric approach using a dye tracer because it is difficult to directly monitor a fluctuating liquid–liquid interface using an optical microscope (Fig. S8†). Our experiment exploits the solvatochromic properties of bromothymol blue (BTB), whereby the dye molecules transition from pale yellow to blue upon transfer from the initial organic phase to a basic NaOH solution (1.0 M; Fig. 1E). We observe that the nanochains self-assemble uniformly at the liquid–liquid interface between the upper ethyl acetate phase and the bottom aqueous phase. In the absence of an applied magnetic field, the stationary nanochains result in the slow and passive diffusion of the BTB tracer (~200 s) from the liquid–liquid interface to the specific endpoint within the lower aqueous phase (Fig. 1F). The application of a rotating magnetic field (100 rpm) facilitates the rapid transfer of BTB molecules to the endpoint within 150 s. Increasing the nanochain spin rate further accelerates the movement of the dye tracer in the aqueous phase, notably reducing the time required for BTB to reach the endpoint to 80 s for spin rates beyond 700 rpm (Fig. S9†). The dependence of BTB movement on the applied magnetic field affirms the importance of nanochain spinning motion in inducing hydrodynamic flows within the bulk solutions for enhanced molecular transfer. Hereon, we refer to the Fe_3O_4@SiO_2 nanochains as interfacial nano-vortexers due to their abilities to spin at the liquid–liquid interface and facilitate the hydrodynamic advection of molecules.

We subsequently apply the interfacial nano-vortexer at the liquid–liquid interface to drive efficient phase-transfer catalysis using the interfacial nitration of phenol as a proof-of-concept demonstration. This reaction holds significant industrial relevance because nitrophenols are critical intermediates for the synthesis of diverse organic compounds, including pharmaceuticals and agrochemicals. It is worth noting that ethyl acetate is selected as the organic phase because it is a well-recognized green solvent in the industry, thereby providing an environmentally friendly alternative to the halogenated solvents commonly used in phase-transfer catalysis. In our reaction setup, the upper ethyl acetate phase contains the phenol reactant and tetrabutylammonium bromide (TBAB; 20 mol%), while the aqueous phase comprises dilute nitric acid (6 wt%) as the nitrating agent. TBAB serves as a phase-transfer catalyst (PTC) facilitating the transfer of polar nitrate ions (NO_3^-) from the aqueous phase into the organic reaction phase *via* a tetrabutylammonium nitrate (TBAN) intermediate (Fig. 2A). The reaction progress is performed at room temperature and monitored using UV-visible absorption spectroscopy, whereby the 2-nitrophenol (2-NP) and 4-nitrophenol (4-NP) products are quantified using their characteristic peak intensity at 349 nm and 315 nm (Fig. 2B and S10†), respectively. Time-dependent UV-visible absorption spectra demonstrate a continuous increase in the peak intensities of 2-NP and 4-NP throughout the 2 hour reaction duration when the interfacial nano-vortexer is subjected to an applied magnetic field rotating at 700 rpm (Fig. 2C and D). Further comparison with pre-constructed calibration curves (Fig. S11†) reveals the rapid formation of 2-NP and 4-NP which eventually reaches a plateau after 120 min. The reaction produces 2-NP and 4-NP at a ratio of ~6 : 4 (Fig. S12†), aligning

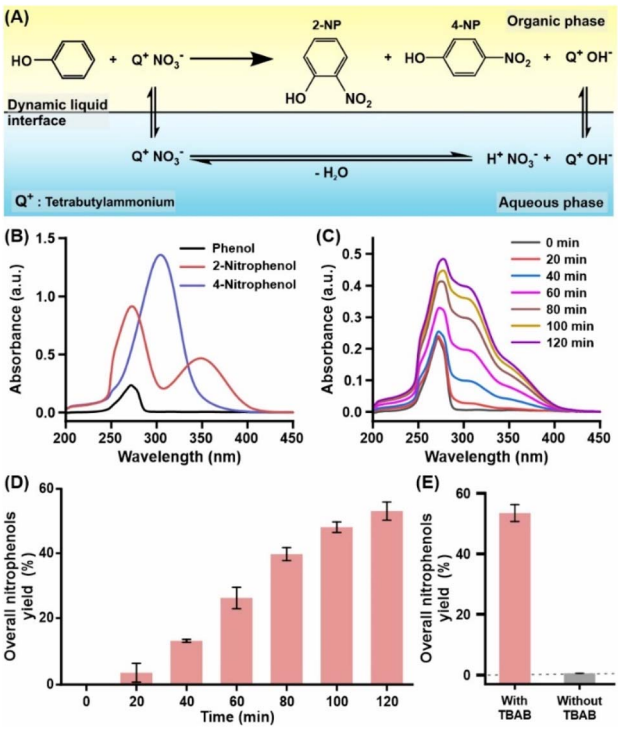

Fig. 2 (A) Reaction scheme demonstrating the nitration of phenol using phase-transfer catalysis and interfacial nano-vortexers. (B) UV-visible absorption spectra of phenol, 2-nitrophenol (2-NP), and 4-nitrophenol (4-NP) in ethyl acetate. (C) UV-visible absorption spectra of the ethyl acetate phase at different reaction times (0–120 min). (D) Time-dependent plot showing the overall nitrophenol yield (includes both 2-NP and 4-NP). The overall nitrophenol yield also indicates the reaction efficiency. (E) Overall nitrophenol yield observed in the presence or absence of TBAB as a phase-transfer catalyst at the end of 120 min. All experiments involve the utilization of an interfacial nano-vortexer.

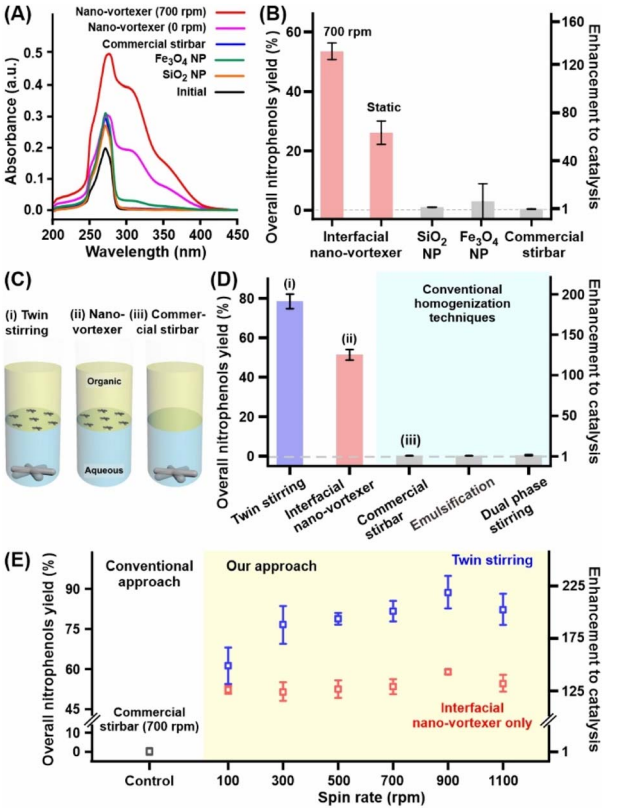

Fig. 3 (A) UV-visible absorption spectra and (B) corresponding overall nitrophenol yield in the ethyl acetate after the interfacial nitration reaction under various reaction conditions. (C) Scheme and (D) overall nitrophenol yield obtained from the interfacial reaction when employing different mass manipulation methods. (E) Overall nitrophenol yield obtained from the interfacial reaction when an applied magnetic field rotates between 100 and 1100 rpm. In (B), (D), and (E), the enhancements in catalysis resulting from various parameters are compared to the conventional approach involving a commercial stirbar rotating at 700 rpm. All reaction duration is for 120 min.

with previous findings reported in the literature. Negligible nitrophenols are produced in the absence of TBAB or nitric acid, thereby affirming the vital roles of these chemicals as the PTC and nitrating agent, respectively, in the interfacial reaction (Fig. 2E and S13†). This observation also implies that the ammonium-based surface chemistry on the interfacial nano-vortexer solely serves to improve the liquid–liquid self-assembly process and does not function as a phase-transfer catalyst.

To identify the unique mass manipulation effects enabled by our design, we perform additional control experiments involving the use of (i) stationary interfacial nano-vortexers, (ii) a commercial stirbar, and the presence of (iii) SiO_2 or (iv) neat Fe_3O_4 nanoparticles at the liquid–liquid interface. All experiments are performed under an applied magnetic field rotating at 700 rpm unless otherwise stated (Fig. 3A). Our spinning interfacial nano-vortexer achieves the highest overall nitrophenol yield and a corresponding reaction efficiency of ~53% (Fig. 3B). This result is >2-fold better than the overall nitrophenol yields obtained from the stationary interfacial nano-vortexer (0 rpm) as well as a biphasic reaction but without any particle at the liquid boundary (Fig. S14†). Control platforms involving SiO_2 or Fe_3O_4 nanoparticles exhibit low overall nitrophenol yields of <4%. Interestingly, the sole use of a commercial stirbar to homogenize the biphasic reaction produces negligible nitrophenols (~0.4%).

Our systematic comparisons jointly highlight five major findings. First, both the SiO_2 and Fe_3O_4 components of the interfacial nano-vortexer do not exhibit catalytic/chemical effects on the interfacial reaction, nor do they facilitate the cross-boundary transfer of catalyst/reactant species *via* adsorption. Second, the alignment of Fe_3O_4 nanoparticles into a chain-like structure is crucial for enabling interfacial stirring. Third, the liquid–solid–liquid interface does not affect the mass transfer of the reactants across the boundary. Fourth, the spinning motion of the interfacial nano-vortexer at the liquid–liquid interface indeed facilitates phase-transfer catalysis, notably through the active converging of biphasic reactants towards the liquid boundary *via* vortex-like hydrodynamic flows. In contrast, the absence of interfacial stirring only allows the passive and random diffusion of chemical species towards the interfacial region which consequently retards the biphasic

reaction. Last and most importantly, conventional stirring of bulk solutions has detrimental consequences on the biphasic reaction. This limitation arises from the use of ethyl acetate as a green organic solvent, in which both the phenol reactant and TBAB PTC have a lower affinity for the organic phase compared to halogenated solvents. As a result, both chemical species are lost to the aqueous phase (*i.e.*, non-reaction phase) which is further exacerbated by the mechanical stirring, thereby deactivating the phase-transfer catalysis. These results evidently underscore the importance of interfacial stirring to effectively manipulate molecule transfer at the liquid–liquid interface, notably enabling a >130-fold enhancement in the catalytic reaction compared to the traditional bulk homogenization approach. Our unique mass manipulation approach thus addresses the formidable challenge in phase-transfer catalysis where catalyst and/or reactant species are easily lost to the non-reaction liquid phase, especially when green solvents are used.

To further enhance the nitration reaction, we employ a unique twin stirring approach that combines nanoscale interfacial stirring through our nano-vortexer with the macroscopic stirring using a commercial stirbar (Fig. 3C). The macroscopic stirring facilitates the swift transportation of reactants and the PTC from the bulk solution to the vicinity of the interfacial region, while the nanoscale interfacial stirring actively pulls these chemical species towards the liquid–liquid interface for chemical reactions. It is worth noting that the interfacial layer of nano-vortexers is highly stable when macroscopic stirring is at 700 rpm (Fig. S15 and S16†), but this layer is eventually disrupted when the rotating magnetic field is further increased to 1100 rpm. Thus, an optimized spin rate of 700 rpm is chosen to ensure maximum catalytic efficiency while maintaining the integrity of the nano-vortexer layer at the liquid–liquid interface. At a standardized spin rate of 700 rpm, our twin stirring approach achieves a high overall nitrophenol yield of ~80% (Fig. 3D) which is ~1.5-fold better than that of a standalone interfacial nano-vortexer. Notably, twin stirring also enhances the interfacial reaction by ~200-fold compared to conventional bulk stirring, even though both methods utilize a commercial stirbar. We also compare our twin stirring to two other conventional homogenization methods involving (1) the violent emulsification of the biphasic system using a mechanical shaker and (2) the concurrent mechanical stirring of both the organic and aqueous phases using an overhead stirrer and commercial stirbar (dual phase stirring), respectively. Interestingly, all three control experiments employing conventional homogenization methods produce negligible nitrophenol with <1% yield. This observation provides concrete evidence that the interfacial nano-vortexer is critical in driving the interfacial reaction. Further temporal studies reveal that the increase in overall nitrophenol yield is relatively similar between twin stirring and standalone interfacial stirring up to ~100 min. However, extending the reaction time to 120 min results in a distinct difference between the two methods (Fig. S17A†). That is, the overall nitrophenol yield for standalone interfacial stirring remains consistent at ~50%, while the twin stirring approach demonstrates a continuous increase in the overall yield to ~80% at 120 min (Fig. S17B†). The poorer performance from standalone interfacial stirring is attributed to the gradual formation of a concentration depletion region near the liquid–liquid interface stemming from the continual consumption of reactants (*e.g.* phenol and nitrate ions) in both the organic and aqueous phases. In this case, the biphasic system relies on slower molecule transportation from the bulk solutions to the vicinity of the liquid–liquid interface. More importantly, the twin stirring approach overcomes this limitation by leveraging macroscopic stirring to homogenize bulk solution and rapidly replenish reactants at the interfacial region for efficient phase-transfer catalysis. This result clearly exemplifies the importance of coupling interfacial nano-vortexers with bulk stirring to effectively manipulate chemical species across the entire biphasic system.

Moreover, the catalytic efficiency of the interfacial reaction can be easily enhanced by controlling the rotational rates of the applied magnetic field for both the twin stirring and standalone interfacial nano-vortexer. With the twin stirring approach, the overall nitrophenol yield experiences a drastic increase from ~0% to ~60% as the spin rate rises from 0 rpm to 100 rpm (Fig. 3E), respectively. Further elevation of the spin rate from 300 rpm to 1100 rpm leads to an even greater enhancement of the interfacial nitration reaction, resulting in a high overall nitrophenol yield ranging from 80% to 90%. The enhanced catalysis at higher spin rates is attributed to the larger centrifugal force generated by the interfacial nano-vortexer, thereby inducing stronger vortex-like hydrodynamic flows to facilitate the biphasic reaction. Conversely, the standalone interfacial nano-vortexer also exhibits improved reaction efficiency as the spin rate increases from 0 rpm to 100 rpm. However, increasing the spin rates beyond 100 rpm does not provide any additional improvement to the interfacial reaction. This observation again highlights the mass transfer limitation in bulk solutions when using a standalone interfacial nano-vortexer such that the interfacial region is not readily replenished with reactants. We thus showcase the unprecedented use of interfacial nano-vortexers and the twin stirring approach to boost biphasic reactions (*e.g.*, phase-transfer catalysis in this case), even when employing ethyl acetate as a green organic solvent. These advantages notably facilitate the efficient (90%) and rapid (2 h) interfacial nitration of phenols through a more sustainable approach, surpassing conventional interfacial methods that typically require a longer reaction duration (~4 h) and environmentally harmful organic solvents (*e.g.*, halogenated solvents such as ethylenedichloride).

From our comprehensive investigations, we infer that the mechanism underlying the interfacial nano-vortexer and twin spinning approach involves the synergistic utilization of nanoscale interfacial spinning and macroscopic stirring to facilitate biphasic reactions (Fig. 4A). The strategic positioning of the nano-vortexer between the immiscible solvents notably results in a dynamic liquid–liquid interface. The interfacial nano-vortexer spins on demand upon exposure to a rotational magnetic field, triggering vortex-like hydrodynamic flows that originate from the spinning objects and extend into both the upper organic phase and bottom aqueous phase. This hydrodynamic phenomenon actively pulls nitrate ions from the

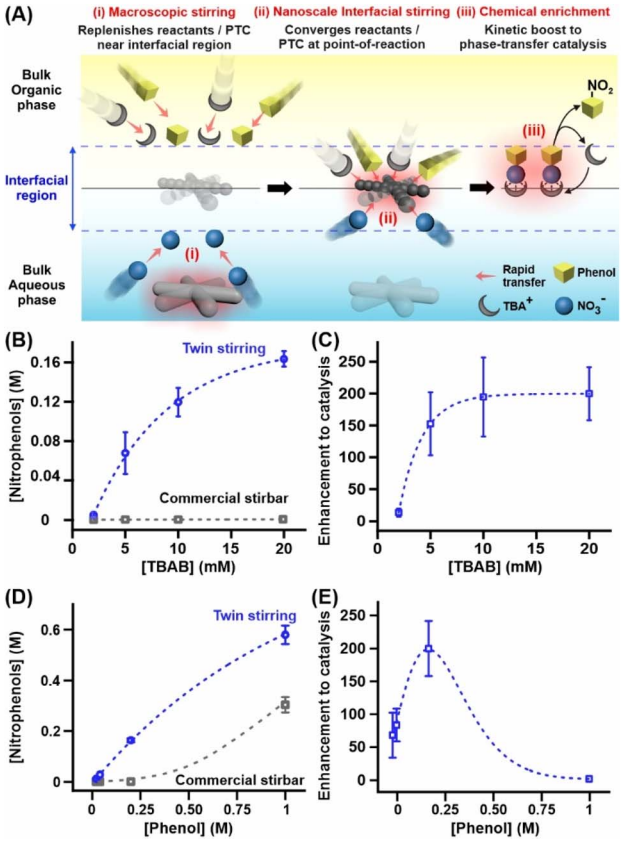

Fig. 4 (A) Proposed mechanism on the mass manipulation effects using the interfacial nano-vortexer and twin stirring. (B) The concentration of nitrophenols formed and (C) the corresponding enhancement in catalysis when employing twin stirring or a commercial stirbar at different TBAB concentrations. (D) The concentration of nitrophenols formed and (E) the corresponding enhancement in catalysis when using twin stirring or a commercial stirbar at various phenol concentrations.

aqueous phase, as well as the phenol substrate and PTC from the organic phase, towards the target liquid–liquid interface. Consequently, the enrichment of reactants, the PTC, and the active TBAN intermediate at the point-of-reaction kinetically enhances the interfacial nitration process in the organic reaction phase. Moreover, the twin spinning method further employs macroscopic stirring to rapidly transport reactant species and the PTC from the bulk solutions to the interfacial region. The combined effect of nanoscale interfacial spinning and macroscopic stirring ensures a constant supply of chemical species and regeneration of the TBAN intermediate at the liquid–liquid interface for continuous phase-transfer catalysis. Our interfacial nano-vortexer and twin spinning approach thus enable an effective and dynamic liquid–liquid interface for boosting biphasic reactions *via* the directional and swift manipulation of chemical species at both the nano- and macroscopic scales. This feat is particularly noteworthy as it overcomes the challenges encountered when using a non-dynamic liquid–liquid interface (*e.g.*, bulk homogenization only at a single phase), where random and passive molecular diffusion dominates in this relatively stationary liquid boundary due to interfacial viscous drag.

We further exploit the unique mass manipulation effects of the interfacial nano-vortexer to enhance phase-transfer catalysis even in the presence of dilute chemical species (*i.e.*, reactants or PTC), especially when utilizing green organic solvents. Achieving this goal is crucial for overcoming the need for high reactant/catalyst concentrations in typical biphasic reactions to promote practical, safer, and more sustainable chemical applications. For instance, phenol is a flammable and highly corrosive chemical that threatens life even at ~250 ppm.[38] We employ the twin stirring approach to maximize catalytic efficiency and compare it to the conventional bulk homogenization method (*i.e.*, standalone commercial stirbar), both operating at 700 rpm. Our focus lies in varying the concentrations of phenol and TBAB because the former is the limiting reactant in the catalysis while the latter is a homogenous phase-transfer catalyst that can be challenging to recover after the reaction. In the case of TBAB, we observe that the twin stirring approach attains an overall nitrophenol yield that increases from ~3% to 88% as the TBAB concentration rises from 2 mM to 20 mM (Fig. 4B and S18†), respectively. Conversely, conventional mechanical stirring produces negligible nitrophenol products (<0.4%) regardless of the initial TBAB concentration. When compared to the standalone commercial stirbar, the twin stirring approach thus enhances phase-transfer catalysis by >10-fold (Fig. 4C) even at low TBAB concentration (2 mM), reaching a maximum of ~200-fold enhancement at higher TBAB concentration (≥10 mM). The observed plateau (≥10 mM) in the catalytic enhancement signifies that the twin stirring approach effectively retains and saturates the TBAB at the interfacial region to drive the catalytic cycle.

Similarly, the twin stirring approach also drastically enhances catalysis by ~60-fold to 200-fold as the phenol concentration increases from 0.02 M to 0.2 M, respectively (Fig. 4D, E and S19†). These enhancements arise due to the negligible formation of nitrophenol at low phenol concentrations (≤0.2 M) when employing conventional mechanical stirring. Further increasing the phenol concentration to 1 M decreases the difference between twin stirring and the conventional approach to <2-fold, indicating that twin stirring exhibits reduced enhancement in catalysis at high phenol concentrations. This phenomenon can be attributed to the abundance of organic reactants near the liquid–liquid interface, where the high phenol concentration partially mitigates the detrimental effects resulting from the inevitable loss of phenol to the aqueous non-reaction phase (Fig. S20†) during standalone bulk stirring. More importantly, the conventional bulk approach clearly requires a high phenol concentration of ~1 M to initiate the interfacial reaction. Our findings collectively reaffirm the ability of the interfacial nano-vortexer and twin stirring to enhance phase-transfer catalysis by enriching phenol and the PTC directly at the point-of-reaction on the liquid–liquid interface. This unique advantage potentially averts the use of high concentrations of homogeneous catalysts and chemical reagents which could incur high costs and pose severe safety hazards. Furthermore, it is worth noting that our

interfacial nano-vortexer can be easily reused for seven cycles while maintaining high and consistent reaction efficiency with a deviation of <7% (Fig. S21†). The platform also exhibits excellent physical and chemical stabilities even after the catalytic reactions (Fig. S22 and S23†).

3. Conclusion

In conclusion, we have demonstrated the successful implementation of spinnable nano-vortexers at the liquid–liquid interface to drive efficient phase-transfer catalysis in the interfacial nitration of phenol with the use of ethyl acetate as a green organic phase. Our strategy harnesses the spinning motion of the interfacial nano-vortexer to generate vortex-like hydrodynamic flows that extend into both the aqueous and organic phases, actively converging biphasic reactants and the PTC onto the liquid boundary for enhanced catalysis. Moreover, the integration of nanoscale interfacial stirring with macroscopic stirring further facilitates the rapid delivery of chemical species from the bulk solution to the vicinity of the interfacial region. The spinning interfacial nano-vortexers notably promote efficient interfacial nitration, achieving an optimal nitrophenol yield of ~90% in only 2 hours and providing a >200-fold enhancement compared to non-dynamic liquid–liquid interfaces and conventional homogenization methods. It is also noteworthy that this approach outperforms previous interfacial designs that require 2-fold longer reaction durations and employ environmentally harmful halogenated organic solvents. More importantly, the ability of the interfacial nano-vortexer to enrich reactants and catalysts at the point-of-reaction is crucial in circumventing the need for high concentrations of homogeneous catalysts and/or chemical reagents, which would otherwise incur high costs and pose severe safety hazards.

Our approach is versatile and can be easily extended to a wide range of molecular transformations and liquid–liquid combinations. We also envision the integration of interfacial nano-vortexers with flow chemistry to expedite its progress towards practical applications. By enabling efficient multiphasic reactions *via* effective mass manipulations at both the nano- and macroscopic scales, our work opens up enormous opportunities to unlock novel and greener chemistries that were previously inaccessible using traditional single-phase reactions. Achieving this will expedite progress towards sustainable and facile molecule transformations under mild conditions useful in diverse chemical, energy, and environmental applications. Potential emerging applications include green chemical manufacturing, waste valorization, chemical/material recovery, environmental remediation, and facile synthesis of chemical fuels.

Author contributions

Z. Z. Ang designed and carried out the experiments, data analysis, and wrote the original manuscript. V. Pereira, S. K. Boong and H. Li took part in the discussion and manuscript review. H. K. Lee provided resources, directed research efforts, and completed the writing – review and editing of the manuscript.

Conflicts of interest

The authors declare no conflict of interest.

Acknowledgements

H. K. L. acknowledges the funding support from the Singapore Ministry of Education (AcRF Tier1 RS13/20 and RG4/21), the A*STAR Singapore (AME YIRG A2084c0158), National University of Singapore Center of Hydrogen Innovation (CHI-P2022-05), and the Nanyang Technological University start-up grants. The research was conducted as a part of NICES (NTU-IMRE Chemistry Lab for EcoSustainability; REQ0275931), a joint research initiative between the Nanyang Technological University (NTU) and the Institute of Materials Research and Engineering (IMRE) from Agency for Science, Technology and Research (A*STAR).

Notes and references

1 X. Zuwei, Z. Ning, S. Yu and L. Kunlan, *Science*, 2001, **292**, 1139–1141.
2 S. Crossley, J. Faria, M. Shen and D. E. Resasco, *Science*, 2010, **327**, 68–72.
3 J. Kaschel, T. F. Schneider and D. B. Werz, *Angew. Chem., Int. Ed.*, 2012, **51**, 7085–7086.
4 D. Dedovets, Q. Li, L. Leclercq, V. Nardello-Rataj, J. Leng, S. Zhao and M. Pera-Titus, *Angew. Chem., Int. Ed.*, 2022, **61**, e202107537.
5 Y. Zhang, Z. Ye, C. Li, Q. Chen, W. Aljuhani, Y. Huang, X. Xu, C. Wu, S. E. J. Bell and Y. Xu, *Nat. Commun.*, 2023, **14**, 1392.
6 M. Zhang, L. Wei, H. Chen, Z. Du, B. P. Binks and H. Yang, *J. Am. Chem. Soc.*, 2016, **138**, 10173–10183.
7 Y. Zhang, R. Ettelaie, B. P. Binks and H. Yang, *ACS Catal.*, 2021, **11**, 1485–1494.
8 M. Pera-Titus, L. Leclercq, J.-M. Clacens, F. De Campo and V. Nardello-Rataj, *Angew. Chem., Int. Ed.*, 2015, **54**, 2006–2021.
9 J. Peng, F. Shi, Y. Gu and Y. Deng, *Green Chem.*, 2003, **5**, 224–226.
10 C. Bertin, C. Cruché, F. Chacón-Huete, P. Forgione and S. K. Collins, *Green Chem.*, 2022, **24**, 4414–4419.
11 M. Ferreira, H. Passos, A. Okafuji, A. P. M. Tavares, H. Ohno, M. G. Freire and J. A. P. Coutinho, *Green Chem.*, 2018, **20**, 1218–1223.
12 M. Jiang, J. Tan, Y. Chen, W. Zhang, P. Chen, Y. Tang and Q. Gao, *Chem. Commun.*, 2023, **59**, 3103–3106.
13 S. K. Au, B. R. Bommarius and A. S. Bommarius, *ACS Catal.*, 2014, **4**, 4021–4026.
14 E. Brenna, M. Crotti, F. G. Gatti, A. Manfredi, D. Monti, F. Parmeggiani, S. Santangelo and D. Zampieri, *ChemCatChem*, 2014, **6**, 2425–2431.
15 Z. Sun, U. Glebe, H. Charan, A. Böker and C. Wu, *Angew. Chem., Int. Ed.*, 2018, **57**, 13810–13814.
16 X. Yan, R. M. Bain and R. G. Cooks, *Angew. Chem., Int. Ed.*, 2016, **55**, 12960–12972.

17 M. Schrimpf, P. A. Graefe, A. Holl, A. J. Vorholt and W. Leitner, *ACS Catal.*, 2022, **12**, 7850–7861.
18 S. Kumar, V. Ahluwalia, P. Kundu, R. S. Sangwan, S. K. Kansal, T. M. Runge and S. Elumalai, *Bioresour. Technol.*, 2018, **251**, 143–150.
19 C. Tang, Y. Chai, C. Wang, Z. Wang, J. Min, Y. Wang, W. Qi, R. Su and Z. He, *Langmuir*, 2022, **38**, 12849–12858.
20 K. Sato, M. Aoki and R. Noyori, *Science*, 1998, **281**, 1646–1647.
21 V. Rauniyar, A. D. Lackner, G. L. Hamilton and F. D. Toste, *Science*, 2011, **334**, 1681–1684.
22 G. Pupo, F. Ibba, D. M. H. Ascough, A. C. Vicini, P. Ricci, K. E. Christensen, L. Pfeifer, J. R. Morphy, J. M. Brown, R. S. Paton and V. Gouverneur, *Science*, 2018, **360**, 638–642.
23 E. J. Corey, F. Xu and M. C. Noe, *J. Am. Chem. Soc.*, 1997, **119**, 12414–12415.
24 T. Ooi, Y. Uematsu, M. Kameda and K. Maruoka, *Angew. Chem., Int. Ed.*, 2002, **41**, 1551–1554.
25 K. Erfurt, M. Markiewicz, A. Siewniak, D. Lisicki, M. Zalewski, S. Stolte and A. Chrobok, *ACS Sustainable Chem. Eng.*, 2020, **8**, 10911–10919.
26 Y. Mahha, L. Salles, J.-Y. Piquemal, E. Briot, A. Atlamsani and J.-M. Brégeault, *J. Catal.*, 2007, **249**, 338–348.
27 R. H. Ingle and N. K. K. Raj, *J. Mol. Catal. A Chem.*, 2008, **294**, 8–13.
28 V. Joshi, M. Baidoosi, S. Mukhopadhyay and Y. Sasson, *Org. Process Res. Dev.*, 2003, **7**, 95–97.
29 N. S. Nandurkar, M. J. Bhanushali, S. R. Jagtap and B. M. Bhanage, *Ultrason. Sonochem.*, 2007, **14**, 41–45.
30 S. Vidal, *ACS Cent. Sci.*, 2020, **6**, 83–86.
31 J. Zhao, Y. Li, G. Yang, K. Jiang, H. Lin, H. Ade, W. Ma and H. Yan, *Nat. Energy*, 2016, **1**, 15027.
32 W. Yue, M. Chen, Z. Cheng, L. Xie and M. Li, *J. Hazard. Mater.*, 2018, **344**, 431–440.
33 R. N. T. Kankanamage, B. K. Ahiadu, J. He and J. F. Rusling, *ChemCatChem*, 2023, **15**, e202300119.
34 X. Li, H. K. Lee, I. Y. Phang, C. K. Lee and X. Y. Ling, *Anal. Chem.*, 2014, **86**, 10437–10444.
35 W. H. Chong, L. K. Chin, R. L. S. Tan, H. Wang, A. Q. Liu and H. Chen, *Angew. Chem., Int. Ed.*, 2013, **52**, 8570–8573.
36 Y. Sánchez-Vicente, C. Pando, M. Cortijo and A. Cabañas, *Microporous Mesoporous Mater.*, 2014, **193**, 145–153.
37 M. Alsalbokh, N. Fakeri, A. A. Rownaghi, D. Ludlow and F. Rezaei, *Chem. Eng. J.*, 2021, **409**, 128277.
38 B. Bukowska and S. Kowalska, *Toxicol. Lett.*, 2004, **152**, 73–84.